JOURNAL OF MATERIALS SCIENCE **40** (2005) 853–859

The influence of annealing twinning on microstructure evolution

V. RANDLE
Materials Research Centre, University of Wales Swansea, Swansea UK
E-mail: v.randle@swansea.ac.uk

This paper reports an experimental investigation on the effect of multiple twinning on the interface population in two low stacking-fault alloys. This is an important topic for grain boundary engineering because annealing twinning is the indirect cause of improved intergranular corrosion resistance in this class of materials. Proportions of $\Sigma 3^n$ ($n = 1$–5) boundaries were analysed in both a brass specimen and a superalloy specimen where the boundaries had been processed so as to be very mobile and less mobile respectively. When $\Sigma 3$ twin boundaries (as distinct from $\Sigma 3$ grain boundaries) are discounted, the $\Sigma 3^n$ distribution for both specimens had a peak at $\Sigma 9$, because $\Sigma 3 + \Sigma 9 \rightarrow \Sigma 3$ occurs more frequently than $\Sigma 3 + \Sigma 9 \rightarrow \Sigma 27$. The distributions and reactions between various $\Sigma 3^n$ values are described and discussed in detail. A novel trace analysis procedure is used to extract information from $\Sigma 3$ boundaries to decide whether or not they are annealing twins, and so provide a convenient means to assess proportions of twin and non-twin $\Sigma 3$s. The data show unambiguously that a significant proportion of $\Sigma 3$s are not on {111}, and these boundaries have on average higher angular deviations from the exact $\Sigma 3$ reference misorientation than do other $\Sigma 3$s. A population of $\Sigma 3$s which were vicinal to annealing twins were also recorded. These data support the contention that profuse annealing twinning produces concurrently many not-twin $\Sigma 3$s, which are pivotal in grain boundary engineering.

1. Introduction

'Grain boundary engineering' refers to the manipulation of interfaces in a polycrystal via processing in order to improve material properties, as originally proposed by Watananbe [1]. Probably the most well-known application of grain boundary engineering is based on the generation of large proportions of annealing twins, which has been shown to confer increased protection against intergranular corrosion [2]. However it is interesting that although annealing twinning is instrumental in the grain boundary engineering process, the twins themselves are not part of the grain boundary network insofar as transport phenomena are concerned, and so the mechanism must involve an indirect effect of twinning. One 'indirect effect' is that the increase in annealing twinning during processing increases concurrently those boundaries which are crystallographically related to twins. These boundaries are, in coincidence site lattice (CSL) notation, $\Sigma 3$ boundaries other than twins and $\Sigma 3^n$ boundaries.

In many investigations which measure grain boundary statistics the categories 'annealing twins' and '$\Sigma 3$' are treated synonymously. This generalisation is not valid because the $\Sigma 3$ designation encompasses annealing twins (which are symmetrical tilt interfaces on the {111} boundary plane), various other symmetrical and asymmetrical tilt and twist boundaries (in practice, mostly asymmetric tilts [3]) and grain boundaries which happen to have a $\Sigma 3$ misorientation but generally have irrational, i.e. random, boundary planes). All these interfaces, although represented by the same misorientation (60°/111) and Σ-value ($\Sigma 3$), are essentially differentiated by their interfacial plane type, which confers upon them markedly different properties. For example 'coherent' annealing twins, on {111}, are almost immobile whereas other tilt and twist types, such as the {112} 'incoherent' twin, have high mobilities. It is therefore confusing when investigating interfacial properties to designate all $\Sigma 3$s, and indeed all Σ-values, in the same category.

An example of an investigation where $\Sigma 3$ grain boundaries are distinguished from twins is in alloy 600 (Ni-16Cr-9Fe) where deformations of 2–5% followed by anneals at 890–940°C for 1–20 h were found to increase the proportion of $\Sigma 3$s and $\Sigma 9$s from 6 to 12% and 5 to 12% respectively, accompanied by a marked improvement in properties [4]. Because the coherent twin boundaries were omitted from the data set, the proportions appear low compared with statistics from other investigations.

In the light of the central role that annealing twinning plays in grain boundary engineering on low stacking-fault energy materials, and the lack of clarity concerning characterisation of the $\Sigma 3$ family, the objective of this paper is to analyse in detail the structure of $\Sigma 3$ interfaces and the interrelationships between twin boundary

derivatives in two low stacking-fault energy materials, chosen because they have unlike processing histories and microstructures. A novel trace analysis procedure is used to extract information from Σ3 boundaries to prove if they are not annealing twins, and so provide a convenient means to assess proportions of twin and non-twin Σ3s.

2. Experimental procedures

The materials investigated were alpha-brass which had undergone iterative strain-recrystallisation processing to produce an enhanced proportion of Σ3 boundaries, and a nickel-based superalloy, PE16, which had been deliberately overaged to produce a high volume fraction of gamma-prime precipitates at grain boundaries. For the brass specimen, five iterations of 25% uniaxial strain followed by a 300 s anneal at 665°C were used to achieve the desired properties. For the superalloy, specimens of commercially heat treated PE16 were annealed in air at 850°C, i.e., 30°C below the gamma-prime solvus, for times of 1 h, 10 h and 100 h. These two specimens were chosen to represent two different processing histories and microstructures.

Both specimens were prepared using standard metallographic techniques concluded by a final polishing step of a few minutes in silica slurry to ensure a good finish for EBSD. An HKL Technology Channel5 EBSD system interfaced to a Philips XL30 SEM operating at 20 kV was used to obtain crystallographic orientation data. Several orientation maps were acquired from each specimen. A 1.25 μm or 0.5 μm step size (grid spacing) was used to map the brass and superalloy specimens respectively. The orientation data were re-expressed as grain boundary misorientation data, initially using the EBSD software. Further processing was carried out using in-house software.

2.1. Data analysis procedures

The misorientation data from individual boundaries were analysed as described below, in order to focus on the interrelationships between twin-related interfaces.

Interactions of twins (which occurs when a twinned portion of grain twins again, or as a result of an encounter between two twin variants) can be described by either multiplication or division of the two Σ-values involved. Where the proportion of Σ3s is high, interactions will occur where twins meet, leading to 'multiple twinning'. This is governed by the following rules to describe the joining or dissociation of CSLs:

$$\Sigma A + \Sigma B = \Sigma(A \times B) \quad (1a)$$

$$\Sigma A + \Sigma B = \Sigma(A/B) \quad (1b)$$

Equation 1b applies only if A/B is an integer and A > B). Hence the meeting of two Σ3s results in either a Σ9 or a Σ1, and if two boundaries at a triple grain junction are Σ3 and Σ9, the third junction is either another Σ3 or a Σ27. In many investigations the proportion of Σ3s is high, whereas the proportion of Σ9s is about one-fifth that of the Σ3s and the proportion of Σ27s is only slightly higher than that for a random distribution [3]. Interactions of this type can theoretically result in twin derivatives $\Sigma 3^n$ in the microstructure and have been shown to be important in the evolution of some recrystallisation textures in fcc materials [5]. 'Twin chains' up to the 6th generation ($n = 6$) have been observed [6]. In the present work proportions of twin derivatives up to the fifth generation, i.e. Σ3, Σ9, Σ27, Σ81 and Σ243, were calculated. The angle/axis pair values (lowest angle solutions) for $\Sigma 3^n$ up to the fifth generation are:

Σ3: 60°/111.

Σ9: 38.9°/110

Σ27: 35.4°/210, 31.6°/110

Σ81: 38.9°/411, 54.5°/322, 38.4°/531, 60.4°/443

Σ243: 43.1°/955, 49.8°/761, 12.2°/311,
35.4°/542, 49.8°/655, 43.1°/971, 31.6°/411,
60.0°/110, 7.4°/110

The fraction of each $\Sigma 3^n$ type was calculated from the orientation map. It should be noted that the fundamental statistic extracted from orientation maps is the length fraction of particular interface types. The number fraction can also be obtained if grains and hence grain boundaries can be identified unambiguously. Depending on the grain structure, there are usually significant differences between the number fraction and the length fraction [7]. For the present work, both length fractions and number fractions were calculated.

The angular tolerance about the exact Σ reference misorientation has traditionally been given by the Brandon criterion [8]. The value of this parameter for Σ3, Σ9, Σ27, Σ81 and Σ243 is 8.7°, 5.0°, 2.9°, 1.7° and 1.0° respectively. Insofar as recognition of 'special' properties is concerned, a more restrictive range than that specified by the Brandon criterion is more appropriate [9], and furthermore only very low Σ values might be associated with special properties. However for the purposes of tracking the distribution and geometrical interactions of $\Sigma 3^n$ boundaries, as in the present case, it is more appropriate to use the larger Brandon criterion.

For the purposes of orientation mapping Σ3 boundaries were categorised according to how close the misorientation was to the exact Σ3 reference of 60°/⟨111⟩. The purpose of this step is that it has been previously shown that annealing twins on {111} are close to the reference misorientation whereas Σ3s which are not annealing twins on {111} are in general displaced from the reference misorientation [10, 11]. For the present work, in the orientation maps Σ3s that are <2° from the reference misorientation, which in general are twins on {111}, are distinguished from those which are >2° from the reference, which in general are Σ3s not on {111}. These classifications were subsequently refined by further trace analysis of a subset of the Σ3 population. This procedure will now be described.

As stated above, the grain boundary plane of true annealing twins is {111} in both interfacing grains. A

relatively simple procedure, which requires no serial sectioning, has been devised to test for {111}, provided that the angle α that the trace of the plane makes with a reference axis in the orientation map can be accurately measured. From a pair of orientations across an interface a misorientation and the proximity to the reference CSL is calculated. Then a crystallographic vector T, the 'trace vector', is obtained in the coordinate systems of both interfacing grains, grain A and grain B, from knowledge of α and the orientation matrix of both grains. Since T lies in the grain boundary plane it is orthogonal to the boundary plane normal vector N, i.e. the following condition applies:

$$N \cdot T = 0 \tag{2}$$

Equation 2 can be used to check if the boundary plane normal is ⟨111⟩ in both grains (i.e. the boundary is a symmetrical $\Sigma 3$ annealing twin on {111}) by substituting ⟨111⟩ for N. On the other hand if N is ⟨111⟩ and the following condition applies in one or both interfacing grains:

$$N \cdot T \neq 0 \tag{3}$$

then it is confirmed that the boundary cannot be a coherent twin on {111} since the plane must contain T. Hence this calculation has the potential to supply partial information about the boundary plane crystallography—what the plane *cannot* be and what it is *likely* to be—without recourse to the more tedious and less accurate full grain boundary plane analysis. The total error in the procedure has been estimated to be less than 2° [12]. More details of the procedure and examples of where it has already been applied are given elsewhere [12–14].

This single-section trace analysis was performed on the superalloy specimen, on 278 straight segments of $\Sigma 3$ interface. Segments of straight $\Sigma 3$ interface which were either very long and/or featured a parallel segment were not included in the analysis since these were expected, from their morphology, to be classical {111} annealing twins.

3. Results

Fig. 1 shows a typical map from the brass specimen. The boundaries are colour coded as follows: low angle boundaries (2°–15°)—dark grey; $\Sigma 3 < 2^\circ$ misorientation—turquoise; $\Sigma 3 > 2^\circ$ misorientation—red; $\Sigma 9$—blue; $\Sigma 27$—yellow; $\Sigma 81$—green; $\Sigma 243$—violet; all other boundaries—black. Similar maps were obtained from the superalloy specimen. The proportion of low angle boundaries present was small in both cases, <1%. Fig. 2 shows the total length proportions of each Σ type. For both specimens the $\Sigma 3$ proportion is by far the greatest, 44.2% for brass and 20.2% for the superalloy specimen. The proportion of $\Sigma 3$ boundaries with misorientations >2° from the $\Sigma 3$ reference is small, <2% of the total interface length. The remaining Σ proportions are an order of magnitude less than that for $\Sigma 3$. The ratio between the $\Sigma 3^n$ classes is almost identical for the brass and superalloy specimens, even though the superalloy specimen contains only half the length proportion of $\Sigma 3^n$ boundaries than does the brass specimen.

It is also instructive to consider the $\Sigma 3$ statistics from the point of view of numbers of boundaries, rather than their length fractions. This is because, for example, a $\Sigma 9$ boundary between two $\Sigma 3$s could be very short, yet it is significant because its presence breaks the continuity of the interface network and so will influence its properties. Fig. 3 shows the $\Sigma 3^n$ statistics in terms of both length and number fraction. On Fig. 3 the very large $\Sigma 3 < 2^\circ$ category, i.e. twins, is omitted so that the other categories, which are present in much smaller quantities, can be seen in more detail. The trend for both the brass and the superalloy is identical: there is a maximum at $\Sigma 9$ (i.e. $n = 2$) and the proportions of higher Σ values ($n = 3, 4, 5$) drop off steadily. The trend is more marked for the number statistics than for the length statistics, indicating the presence of a large number of small segments of the various interfaces, particularly $\Sigma 9$. Fig. 4 is a small portion of one of the maps from the superalloy, enlarged so that details of the interface network are visible. This portion has been chosen because it illustrates a variety of $\Sigma 3^n$, rather than because it is a typical region. In fact, the proportion of $\Sigma 3 > 2^\circ$ and $\Sigma 81$ boundaries is higher than average in this area. Many segments of $\Sigma 3^n$ interface generated according to the crystallographic relationship in Equation 1 are discernible in Fig. 4, for example $\Sigma 3/\Sigma 3/\Sigma 9$, $\Sigma 3/\Sigma 27/\Sigma 81$, $\Sigma 9/\Sigma 9/\Sigma 81$ and $\Sigma 3/\Sigma 81/\Sigma 243$. These examples are labelled 1 to 4 respectively on Fig. 4. The $\Sigma 3 > 2^\circ$, $\Sigma 9$, $\Sigma 27$, $\Sigma 81$ and $\Sigma 243$ segments are mostly short compared to both $\Sigma 3 < 2^\circ$ boundaries (turquoise) and general grain boundaries (black). This characteristic is also apparent on Fig. 1.

The remaining part of the data to be reported here pertains to the crystallography of $\Sigma 3$s in the superalloy where the trace angle was measured, and hence the boundary plane was tested for if it was *not* {111}. The critical experimental parameters are t_A and t_B, the angles between T and ⟨111⟩ in both neighbouring grains A and B respectively. For an exact {111} twin, $t_A = t_B = 90^\circ$. Three groups were identified:

1. $\Sigma 3$s where *both* t_A and t_B were >88° and the deviation from the reference misorientation was <2°. For these cases the boundary was very likely to be on {111}.
2. $\Sigma 3$s where *both* t_A and t_B were 80–88° and the deviation from the reference misorientation was <2°. For these cases the boundary was very likely to be vicinal to {111}.
3. $\Sigma 3$s where the average value of t_A and t_B was <80°. For these cases the boundary was definitely not {111}.

Based on the criteria listed above, in the sample population 31% of boundaries were {111} (group 1), 39% were vicinal to {111} (group 2) and 30% were not {111} (group 3). It must be realised that these statistics do not reflect the *overall* proportions in the specimen, only those in the sample population. The sampling was necessarily highly biased because some $\Sigma 3$s did not have a

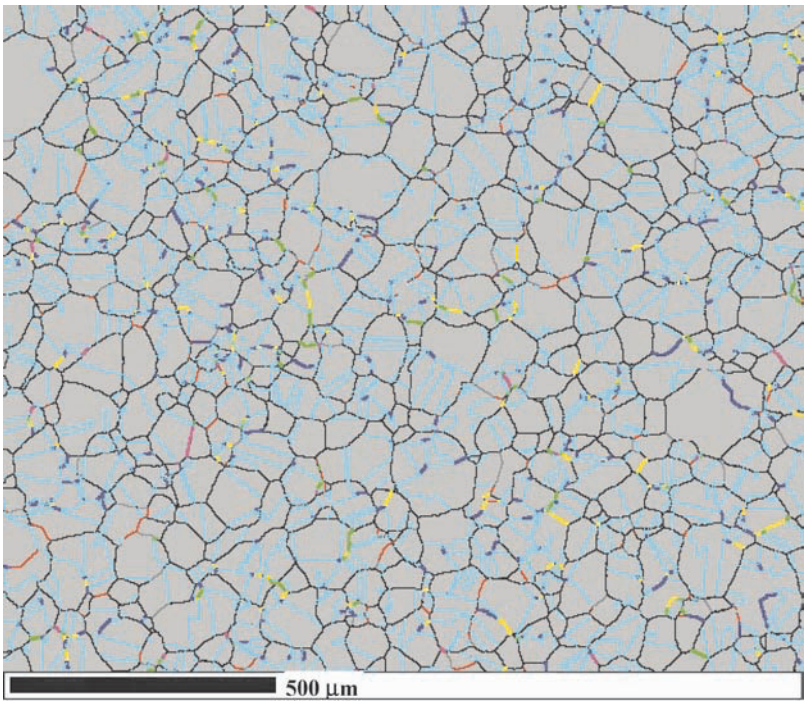

Figure 1 Orientation map from brass, acquired with a step size of 2.5 μm. Interfaces are colour coded as follows: low angle boundaries (2°–15°): dark grey; $\Sigma 3 < 2°$ misorientation—turquoise; $\Sigma 3 > 2°$ misorientation—red; $\Sigma 9$—blue; $\Sigma 27$—yellow; $\Sigma 81$—green; $\Sigma 243$—violet; all other boundaries—black. The background to the map had been shaded a uniform light grey.

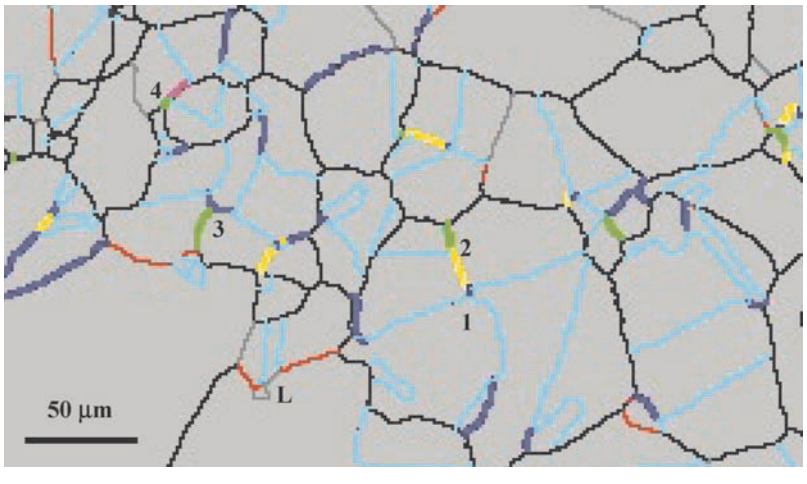

Figure 4 Enlarged portion of a map from the superalloy, acquired with a step size of 0.5 μm. Interfaces are colour coded as in Fig. 1. Five triple junctions are labelled. They are categorised according to their constituent grain boundaries as follows: 1: $\Sigma 3/\Sigma 3/\Sigma 9$; 2: $\Sigma 3/\Sigma 27/\Sigma 81$; 3: $\Sigma 9/\Sigma 9/\Sigma 81$; 4: $\Sigma 3/\Sigma 81/\Sigma 243$; L: $\Sigma 3/\Sigma 3/\Sigma 1$.

sufficiently well defined straight segment for measurement purposes, and those $\Sigma 3$s with the typical twin morphology were omitted for economy of effort.

Group 2 has been included in its own right because previously in many experimental investigations to measure the plane crystallography of $\Sigma 3$s a large group of boundaries vicinal to {111} has been observed [3, 10, 12]. These boundaries are usually symmetrically displaced from {111} along the 011 zone. Other vicinal boundaries have also been observed [15]. The vicinal group here is distinctive from the non-{111} group (group 3) in that the 'difference angle' between t_A and t_B is small for the former, indicating symmetrical displacement from {111}, whereas the difference angle between t_A and t_B is frequently large for group 3. The average difference angles are listed in Table I, and the distribution of difference angles between t_A and t_B for the {111} and vicinal-to-{111} groups are shown on Fig. 5. It is seen that the average difference angle (0.4°) is skewed towards zero for the {111} group, slightly higher (0.8°) for the vicinal-to-{111} group, and an order of magnitude higher (10.0°) for the not-{111} group. It is possible

TABLE I Measured parameters of the $\Sigma 3$ population

Group	Average difference angle between t_A and t_B (°)	Mean deviation from $\Sigma 3$ reference (°)	Standard deviation (°) of mean
1. {111}	0.4	0.52	0.06
2. Vicinal-to-{111}	0.8	0.52	0.12
3. Not-{111}	10.0	2.0	0.31

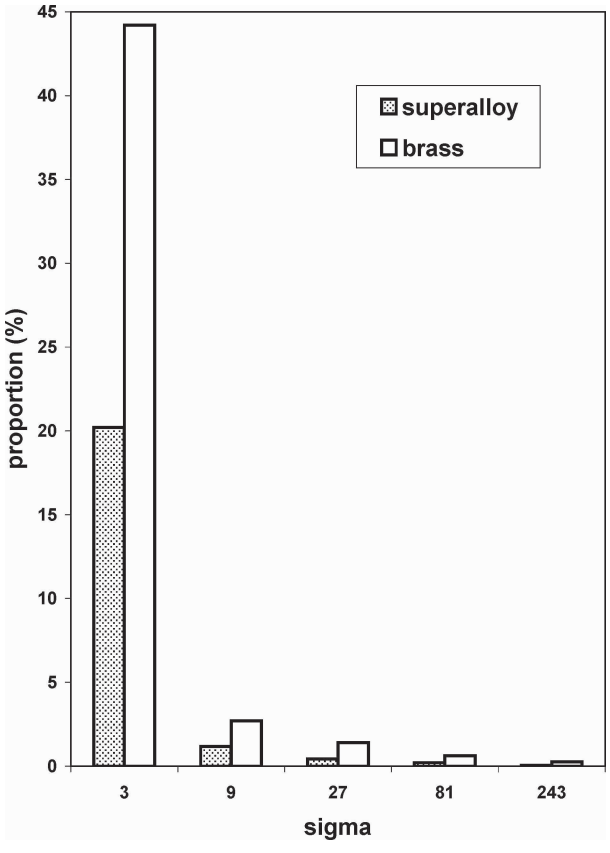

Figure 2 Proportions of $\Sigma 3^n$ boundaries in both the superalloy and the brass specimens.

that experimental errors have resulted in a small proportion of the vicinal-to-{111} group being mistakenly classified. However the experimental method is robust, and few mistaken classifications are expected.

The mean deviation from $\Sigma 3$ misorientation for the three groups and the standard deviation of the mean are also shown in Table I. The mean deviation from $\Sigma 3$ misorientation is higher for the not-{111} group than for the other two groups. The standard deviation of the mean further reveals that the {111} group has very little variation about the mean, the vicinal-to-{111} group show more variation and the not-{111} shows the highest variation.

4. Discussion

It is clear from the $\Sigma 3^n$ statistics shown in Fig. 2 that for both the brass and the superalloy specimens $\Sigma 3^n$ boundaries do not build up in either of the microstructures. Even though there are more than double the length fraction of twins in the brass specimen than in the superalloy specimen, the length fractions of $\Sigma 3^n$ grain boundaries in each is practically identical. The number fraction is consistently higher than the length fraction (Fig. 3), but more importantly there is a much more significant peak at $\Sigma 9$ in terms of numbers of boundaries than in terms of total grain boundary length. This observation implies that there are large numbers of short $\Sigma 9$ segments in the microstructure, which would be expected given the large twin population, since $\Sigma 3 + \Sigma 3 \rightarrow \Sigma 9$.

For $\Sigma 3$, there are four possible variants of $60^\circ/\langle 111 \rangle$ having the same rotation angle but different rotation axes, namely [111], [-111], [1-11] and [-1-11]. When two twins having *different* rotation axes meet, a $\Sigma 9$ boundary is formed. On the other hand when two twins having the *same* rotation axis meet, a low angle boundary results. An example is labelled L on Fig. 4. There are twelve and four combination possibilities for different and same rotation axes respectively. On this basis alone three times as many $\Sigma 9$ boundaries as low angle boundaries resulting from twin interactions are forecast. However there is not a high incidence of these $\Sigma 9$ segments conjoining other $\Sigma 3$s to produce $\Sigma 27$ according to $\Sigma 3 + \Sigma 9 \rightarrow \Sigma 27$; the proportion of $\Sigma 27$s drops compared to the $\Sigma 9$ proportion. Instead, $\Sigma 3 + \Sigma 9 \rightarrow \Sigma 3$ occursmore frequently,

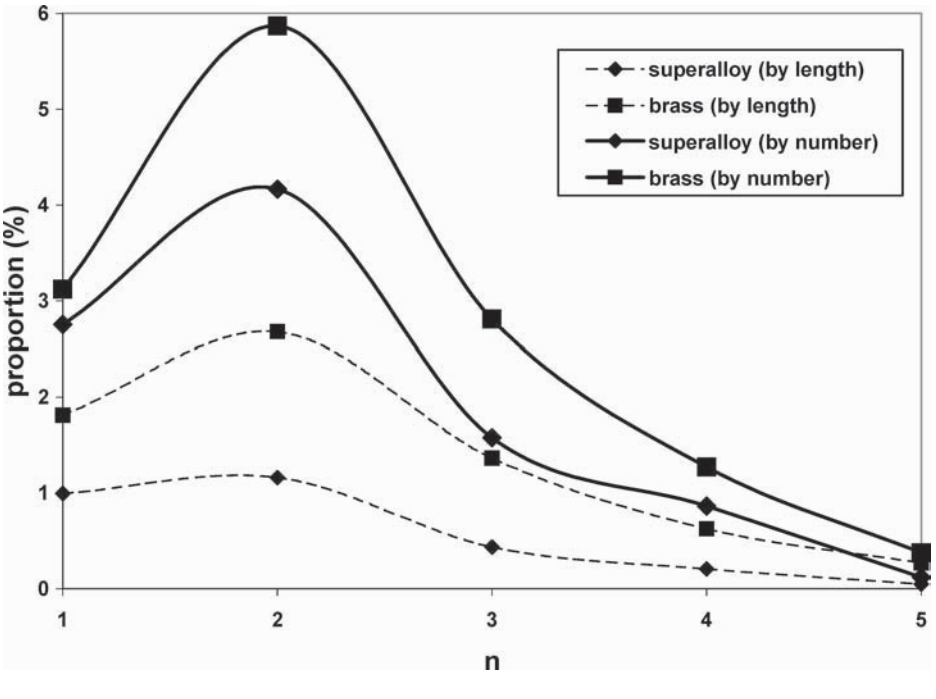

Figure 3 Length fraction and number fraction statistics of $\Sigma 3^n$, where only $\Sigma 3 > 2^\circ$ from the reference misorientation are counted, in both the superalloy and the brass specimens.

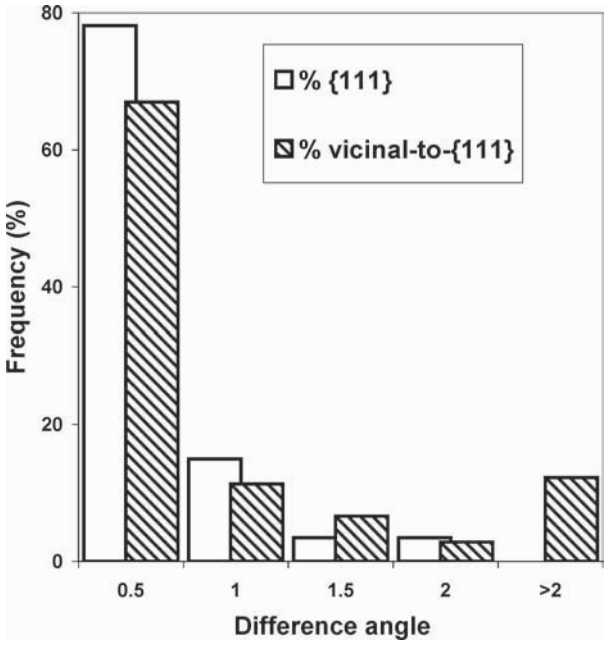

Figure 5 Average difference angle between t_A and t_B for the {111} and vicinal-to-{111} groups. (See text for details.)

which shows that some preferential variant selection is operating.

An interesting feature of the $\Sigma 3^n$ misorientation statistics is that the relative proportions are identical in both the superalloy and the brass, despite that the two materials have undergone totally different processing. Essentially, the brass processing has involved much movement of interfaces because the specimen has been partially recrystallised five times to 'grain boundary engineer' the material. By contrast, interfaces in the superalloy specimen have remained almost immobile because they have been strongly pinned by carbides and the gamma-prime phase [16]. The observation that the proportions of $\Sigma 3^n$ boundaries are higher in brass than in the superalloy is therefore connected with a higher driving force for boundary migration in the brass specimen, compared to strong boundary pinning in the superalloy. In the brass specimen the key mechanism which is controlling the $\Sigma 3^n$ distribution is that $\Sigma 9$s interact with other $\Sigma 3^n$ boundaries to replenish $\Sigma 3$ boundaries in the microstructure according to $\Sigma 3^n + \Sigma 3^{n+1} \rightarrow \Sigma 3$, the '$\Sigma 3$ regeneration model' [3]. This mechanism operates in the both the superalloy and the brass specimens, but at a restricted level in the superalloy specimen because pinning forces reduces boundary mobility, producing fewer impingements. However because there is only half the length fraction of twin boundary present in the superalloy than in the brass, the relative proportions of $\Sigma 3^n$ types turns out to be the is the same for both alloys.

The single-section trace analysis of $\Sigma 3$ boundaries in the superalloy has confirmed that a significant number of $\Sigma 3$ boundaries do not have {111} planes, and are therefore not annealing twins. Furthermore, there is a correlation between the not-{111} and a high average deviation from the $\Sigma 3$ reference, which validates the dual $\Sigma 3$ classification which was used to categorise the misorientation data presented here in the orientation maps and in Figs 2 and 3. Not-{111} $\Sigma 3$s are either grain boundaries because of the contiguity of grains which happen to have a $\Sigma 3$ relationship, or 'incoherent twins', or because of impingement reactions of the type described above, including the $\Sigma 3$ regeneration model. A newly regenerated $\Sigma 3$ from an interaction between two $\Sigma 3^n$ boundaries does not generally inhabit a {111} plane [3]. However because {111} $\Sigma 3$s occupy a markedly low energy position, after formation of a new $\Sigma 3$ there is a driving force for it to reorient as close as possible to {111}. It is suggested that this is one reason for the occurrence of the population of vicinal-to-{111} $\Sigma 3$s. The results from the trace analysis therefore support the conclusion that the formation of $\Sigma 3$ boundaries in the microstructure is by a regeneration reaction, and furthermore supports the contention that profuse annealing twinning produces concurrently many not-twin $\Sigma 3$s, which are pivotal in the grain boundary engineering process.

5. Conclusions

Proportions of $\Sigma 3^n$ ($n = 1$–5) boundaries have been analysed in both a brass specimen and a superalloy specimen where the boundaries have been processed so as to be 'very mobile' and 'less mobile' respectively. When $\Sigma 3$ twin boundaries (as distinct to $\Sigma 3$ grain boundaries) are discounted, the $\Sigma 3^n$ distribution for both specimens has a peak at $\Sigma 9$, because $\Sigma 3 + \Sigma 9 \rightarrow \Sigma 3$ occurs more frequently than $\Sigma 3 + \Sigma 9 \rightarrow \Sigma 27$. Although there are twice as many of each $\Sigma 3^n$ class in the brass specimen than in the superalloy specimen, the relative proportions of $\Sigma 3^n$ are the same. This is because impingement of twin boundaries has been restricted by low boundary mobility in the superalloy specimen, resulting in the same $\Sigma 3^n$ distribution profile for both specimens.

A novel trace analysis methodology has been used to assess whether or not $\Sigma 3$ boundaries are on {111}. The data show unambiguously that a significant proportion of $\Sigma 3$s are not on {111}, and these boundaries have on average higher angular deviations from the exact $\Sigma 3$ reference misorientation than do other $\Sigma 3$s. There is also a population of $\Sigma 3$s which has planes vicinal to {111}. These results support the existence in the microstructure of $\Sigma 3$s which are not annealing twins, introduced by mechanisms such as $\Sigma 3 + \Sigma 9 \rightarrow \Sigma 3$.

References

1. T. Watanabe, *Res. Mech.* **11** (1984) 47.
2. M. SHIMADA, H. KOKAWA, Z. J. WANG, Y. S. SATO and I. KARIBE, *Acta Mat.* **50** (2002) 2331.
3. V. RANDLE, *ibid.* **47** (1999) 4187.
4. D. C. CRAWFORD and G. S. WAS, *Met. Trans.* **23A** (1992) 1195.
5. G. GOTTSTEIN, *Acta Met.* **32** (1984) 1117.
6. P. J. WILBRANDT and P. HAASEN, *Z. Metallk.* **71** (1980) 273.
7. V. RANDLE, *Inter. Sci.* **10** (2002) 271.
8. D. G. BRANDON, *Acta Met.* **14** (1966) 1479.
9. G. PALUMBO and K. T. AUST, *Acta Met. Mat.* **38** (1990) 2343.
10. V. RANDLE, *Acta Mat.* **46** (1997) 1459.

11. V. RANDLE, P. DAVIES and H. DAVIES, in "Proc. ICOTOM12," edited by J. A. Szpunar (NRC Research Press, Canada, 1999) p. 1196.
12. V. RANDLE and H. DAVIES, *Ultramicroscopy* **90** (2002) 153.
13. V. RANDLE, *Scripta Mat.***44** (2001) 2681.
14. S. I. WRIGHT and R. J. LARSEN, *J. Microsc.* **205** (2002) 245.
15. I. MACLAREN and M. AINDOW, *Philos. Mag.* **76A** (1997) 871.
16. V. RANDLE and B. RALPH, *Acta Met.* **34** (1986) 891.